Layer Structures. 5. Influence of the Spacer Length on the Smectic Phases of Poly(ester imide)s Derived from α,ω-Alkane Bis(trimellitimides) and 4,4′-Dihydroxybiphenyl

Hans R. Kricheldorf* and Volker Linzer

Institut für Technische und Makromolekulare Chemie der Universität, Bundesstrasse 45, D-20146 Hamburg, FRG

Mark Leland and Stephen Z. D. Cheng

Maurice Morton Institute and Department of Polymer Science, The University of Akron, Akron Ohio 44325-3909

Received June 25, 1997; Revised Manuscript Received April 25, 1997[⊗]

ABSTRACT: A series of homopoly(ester imide)s, PEIs, was prepared by polycondensation of 4,4′-bis-(acetoxybiphenyl) with the bis(trimellitimides) of α,ω-diaminoalkanes with 6−12 CH_2 groups. Furthermore, a series of copoly(ester imide)s was prepared from equimolar mixtures of 1,12-diaminodocedane bis(trimellitimide) and the bis(trimellitimides) of shorter α,ω-diaminoalkanes. As indicated by well-developed bâttonet textures all homopolyesters form a smectic-A phase before the isotropization. However, wide angle X-ray scattering measurements with synchrotron radiation up to 400 °C suggest that all PEIs also form a smectic-C phase above the melting temperature (T_m). The homopolyesters with an even number of CH_2 groups have mesogens in upright position in the solid state (smectic-E), whereas the mesogens of the homo PEIs with odd-numbered spacers are tilted relative to the layer plane. WAXS fiber patterns demonstrate that in oriented samples the chain axes may adopt a parallel or perpendicular orientation relative to the draw direction. Also most coPEIs form a smectic-A phase in the melt, but when the difference of the spacer lengths increases (e.q. 6+12 and 5+12 CH_2 groups), the layer structure is destabilized and a nematic melt is formed. A fiber drawn from the nematic melt of PEI 6+12 (**2g**) shows the chain axis parallel to fiber axis, whereas in the case of PEI 5+12 (**2h**) the chain axis is perpendicular to the fiber axis.

Introduction

In a previous paper[1] we have reported on the synthesis and properties of poly(ester imide)s, PEIs, built up from α,ω-diaminoalkanes, trimellitic anhydride, and 4,4′-dihydroxybiphenyl (structure **1a**−**i**). Analogous PEIs derived from hydroquinone or 2,6-dihydroxynaphthalene have also been described.[2] These PEIs were the first examples of thermotropic homopolymers containing imide mesogens and they were the first examples of smectic polyimides.[3] More recently the PEIs **3a** and **3b** have been studied, and in both cases an enantiotropic smectic-A phase has been found.[4] Due to the lack of sufficient X-ray measurements at elevated temperatures and due to lack of experience in the characterization of textures the smectic phases of the PEIs **1a**−**i** were not clearly characterized. Therefore, the present work was aimed at studying the layer structures of PEIs **1a**−**i** in more detail and to extend these studies to the copoly-(ester imide)s **2a**−**h**. The combination of two spacers of different length in a random copolymer should destabilize the layers, and the consequences of this destabilization should be elucidated. Analogous studies dealing with two different classes of smectic poly(ester imide)s have recently been reported.[5,6] The influence of a combination of incommensurable spacers on the layer structures was quite different for both classes of poly(ester imide)s. Therefore, the results of the present study were unpredictable.

Nematic copolyesters derived from 4,4′-dihydroxy-α,α′-dimethyl benzalazine and two different alkanediol spacers were studied by Roviello and Sirigu,[7] but those copolyesters did not form layer structures. Copolyesters containing two different oligoethylene glycol spacers and forming a smectic-LC phase were reported by Koide et al.[8] However, the layer structures of the solid state were not analyzed and discussed. LC−copoly(ether esters) containing random sequences of two different spacers were also studied by Kwon and Chung.[9] Yet, those authors concentrated on the mechanical properties of fibers, and layer structures were not discussed. Smectic polyesters with so-called "frustrated layer structures" made up by an alternating sequence of two different spacers have been studied by Watanabe and coworkers[10,11]. Due to the alternating sequences the structure-property relationships of those polyesters are not comparable with those of the present work. However, Watenabe and Krigbaum[12] have also studied the phase behavior of the copolyesters **4a**−**d**,which partially resemble the copoly(ester imide)s **2a**−**h** with regard to both structure and properties.

Experimental Section

Materials. All α,ω-diaminoalkanes and the 4,4′-dihydroxybiphenyl were purchased from Aldrich Co. (Milwaukee, WI). The trimellitic anhydride was a gift of Bayer AG (Leverkusen, Germany). The α,ω-diaminoalkane bis(trimellitimides) were prepared as described previously.[1] The 4,4′-dihydroxybiphenyl was acetylated with an excess of acetic anhydride and a catalytic amount of pyridine in refluxing toluene.

Polycondensation. α,ω-Diaminoalkane bis(trimellitimide) (10 mmol), 1,12-diaminododecane bis(trimellitimide) (10 mmol), 4,4′-bis(acetoxybiphenyl) (20 mmol), and MgO (10 mg) were weighed into a cylindrical glass reactor equipped with a mechanical stirrer gas-inlet and gas-outlet tubes. The reactor was placed into an oil bath preheated to 250 °C. This temperature was maintained for 0.5 h; the temperature was then raised to 280 °C for 0.5 h and kept at 320 °C for 2 h. The liberated acetic acid was removed with a slow stream of nitrogen, but during the last 20 min vacuum was applied. The

[⊗] Abstract published in *Advance ACS Abstracts,* July 15, 1997.

S0024-9297(96)00921-7 CCC: $14.00

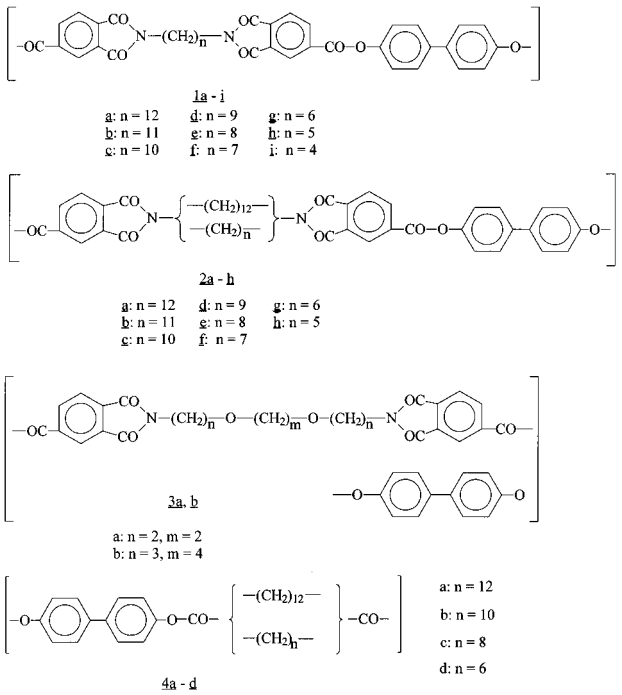

cold product was dissolved in a CH_2Cl_2/trifluoroacetic acid mixture (volume ratio 4:1), precipitated into methanol, and dried at 120 °C. The yields and some properties of the isolated PEIs are summarized in Table 1.

Measurements. The inherent viscosities were measured with an automated Ubbelohde viscometer thermostated at 20 °C.

The wide angle X-ray diffraction (WAXD) powder patterns were recorded with a Siemens D-500 diffractometer using Ni-filtered Cu Kα radiation. The synchrotron radiation measurements were conducted at a wavelength of 1.50 Å at HASYLAB, DESY (Hamburg). A position sensitive, one-dimensional detector was used, and a heating rate of 20 °C/min was applied.

The fiber patterns were recorded with a pinhole camera from fibers drawn by hand from the melt of the corresponding poly(ester imide)s. All computer modeling was conducted with a workstation IBM RS 6000 and software of BiosymTechn. The force field programs Discover V 2.8.0 and DMd V 3.0 (Insight II 2.2.0) were used.

Results and Discussion

Homopoly(ester imide)s. When the textures of the homo PEIs **1a**−**h** were examined for the first time,[1] they looked between crossed polarizers like an assembly of colorful grainy textures, and thus were called "sandy"

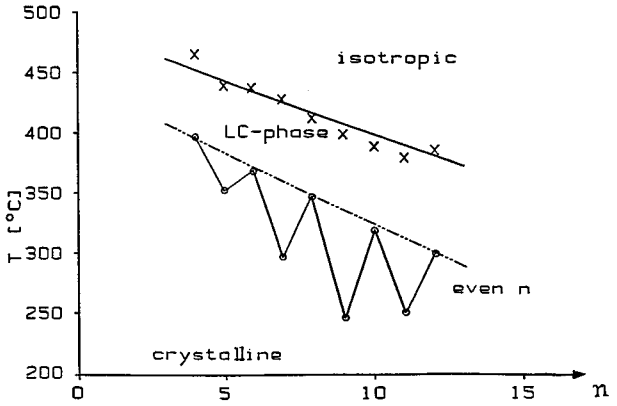

Figure 1. Plot of melting temperatures (T_{m1} from DSC curves) and isotropization temperatures (T_i from opt. microscopy) of the homo-PEIs **1a**−**h**.

textures. In this work the texture were more intensively studied in the temperature range around and immediately below the isotropization temperature (T_i). Due to the high isotropization temperatures (Figure 1) and the limited thermostability above 350 °C these studies were only feasible in the case of **1a**−**f**. In all these cases a bâttonet texture such as that of Figure 2A was observed upon slow cooling from the isotropic melt. The birefringent bâttonets smear out upon shearing between the glass plates and relax when the shearing is stopped. Such a texture is an unambiguous indicator if a smectic-A phase, in as much, as a LC main chain polymer can only form two mobile smectic-LC phases, namely, smectic-A and smectic-C. All higher ordered smectic phases are solid mesophases, in contrast to LC side chain polymers. The existence of a mobile smectic phase was confirmed by X-ray measurements with synchrotron radiation up to 400 °C (ref 1 and discussion below).

As demonstrated previously,[1] the wide angle X-ray spectroscopy (WAXS) powder patterns of **1a**−**h** display a sharp middle angle reflection (MAR) along with its higher order reflections. These reflections indicate the existence of a rather perfect layer structure and allow the calculation of the layer distances (*d*-spacings) via the Bragg equation. A plot of these *d*-spacings versus the number of CH_2 groups gave interesting information (Figure 3). The slope of the plot for even-numbered spacers amounts to 1.13 Å per CH_2 group, which is closer to the value of an all-trans conformation (1.27 Å) than to the value of an all-gauche conformation (0.9 Å)

Table 1. Yields and Properties of the Copoly(ester imide)s 2a−h

polym. no.	*n*	yield (%)	η_{inh}[a] (dL/g)	elemental formula (formula weight)	elemental analyses	C	H	N
2a	12	93	insol	$C_{42}H_{38}N_2O_8$	calcd	72.13	5.48	4.01
				(698.77)	found	72.17	5.63	3.97
2b	11	90	0.72	$C_{83}H_{74}N_4O_{16}$	calcd	72.00	5.39	4.05
				(1383.51)	found	71.11	5.61	4.39
2c	10	94	0.70	$C_{82}H_{72}N_4O_{16}$	calcd	71.92	5.30	4.09
				(1369.49)	found	70.94	5.46	4.33
2d	9	84	0.69	$C_{81}H_{70}N_4O_{16}$	calcd	71.72	5.21	4.13
				(1355.47)	found	71.08	5.39	4.37
2e	8	98	0.72	$C_{80}H_{68}N_4O_{16}$	calcd	71.63	5.11	4.18
				(1341.45)	found	70.69	5.20	4.44
2f	7	87	0.54	$C_{79}H_{66}N_4O_{16}$	calcd	71.42	5.01	4.22
				(1327.43)	found	70.49	5.08	4.40
2g	6	96	0.65	$C_{78}H_{64}N_4O_{16}$	calcd	71.33	4.91	4.27
				(1313.41)	found	70.30	5.07	4.48
2h	5	84	0.59	$C_{77}H_{62}N_4O_{16}$	calcd	71.18	4.81	4.31
				(1299.39)	found	70.22	4.98	4.56

[a] Measured at 25 °C with c = 2 g/L in CH_2Cl_2/trifluoroacetic acid (volume ratio 4:1).

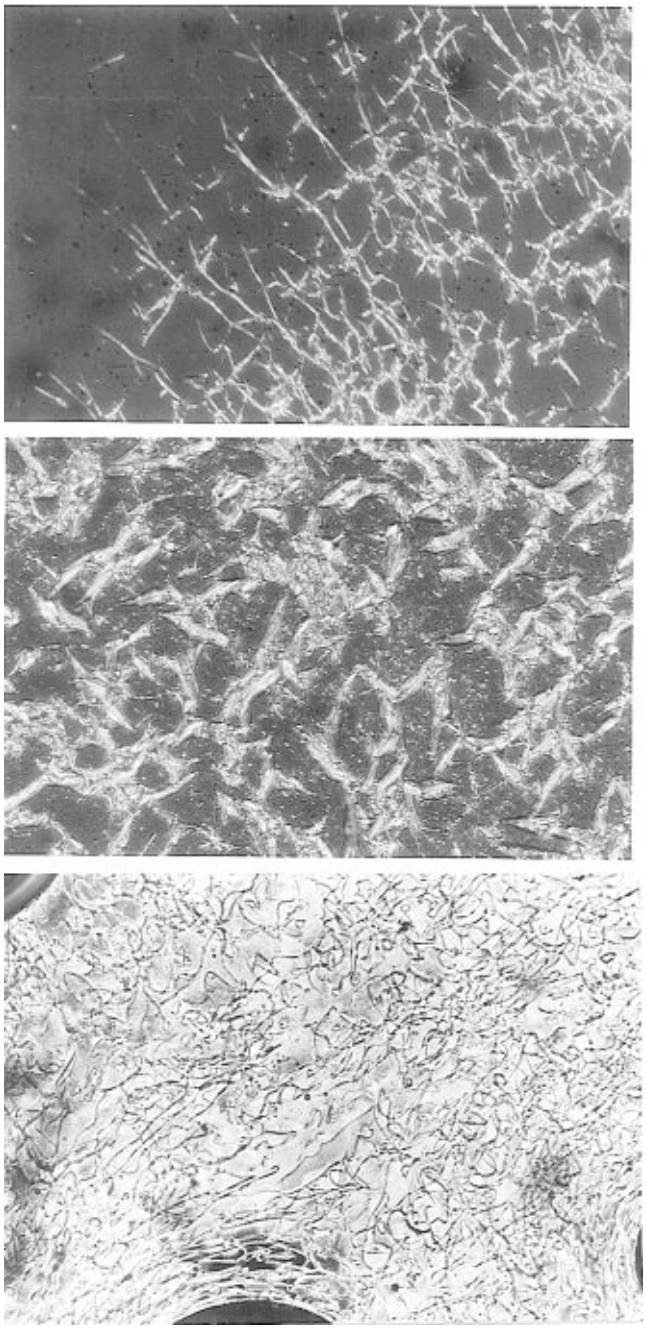

Figure 2. Textures observed around 320−330 °C upon cooling from the isotropic melt: (A) PEI **2a** or **2c**; (B) PEI **2b**; (C) PEI **2g**.

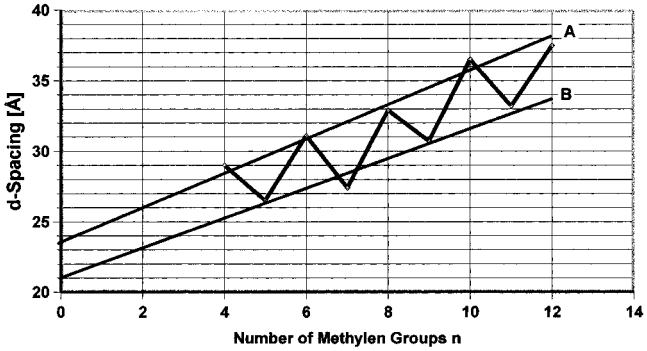

Figure 3. Plot of *d*-spacings versus the number of methylene groups for the homo PEIs **1a**−**h**.

of an alkane chain. This means, the spacers contain slightly more trans than gauche conformations. This interpretation assumes mesogens and spacers to form a straight line (tilt angle 180°). A smaller tilt angle and an all-trans conformation is, of course, not excluded by the WAXS measurements but is thermodynamically unfavorable. The pitch of the odd-numbered spacers seems to be somewhat flatter, corresponding to a higher ratio of gauche (g) and trans (t) conformations (with no tilt between spacer and mesogen) or a greater tilt with low g/t ratio. Unfortunately, the spacers are too short for a detemination of their conformation by ^{13}C NMR cross polarization magic angle spinning spectroscopy.

The extrapolation of the *d*-spacings against CH_2 groups yields an apparent length of the mesogenic unit of 23.4 Å for the even-numbered spacers and a value of 21.0 Å for the odd-numbered PEIs. Computer-modelling with a force field program yielded a maximum length of the mesogen (from N to N plus one σ-bond) of 23.2 Å. Hence, it may be concluded that the mesogens have an upright position relative to the layer plane, when the number of CH_2 groups is even. However, a slight tilting (less than speculated previously[1] may be assumed for the mesogens of PEIs with odd-numbered spacers. This assumption was confirmed by a fiber pattern of PEI **1d** (Figure 4). This fiber pattern indicates that the layer planes exactly parallel the fiber axis, so that the polymer chains are more or less in a perpendicular position. The maximum in the intensity along the azimuthal angle of the wide angle reflection occurs in quadrant suggesting an arrangement in which the mesogens are tilted at an angle with respect to the layer.

Interestingly, the wide angle reflection is much more diffuse than those of the layer. The diffuse character of this reflection is consistent with the orientation of symmetric domains in the fiber-forming process. A detailed and more quantitative explanation of this type of orientation and its respective patterns will be forthcoming in the literature.[13] Briefly, a lateral reflection, (*hk*0), of a system in which the normal to the layer is confined to a direction perpendicular to the fiber axis defines a spherical reciprocal construct in which there is a greater surface density of points in and near the direction of preferred orientation for the molecules. This unusual reciprocal construct results from symmetrization around both the fiber and layer normal axes when the only condition placed on the system is confinement of the normal to the layer in a direction perpendicular to the flow direction. On the basis of intersection of the construct and the sphere of reflection, the resulting pattern is expected to show a maximum in the intensity along the azimuthal angle at the angle describing the tilt between the mesogens and the layers. The expected fiber pattern is further complicated by the presence of the amorphous halo as well as imperfect orientation of the layer. These factors in conjuction with the atypical symmetry of the reciprocal construct suggest that the intensity of the (*hk*O) reflection should not decay to zero anywhere along the azimuthal angle. Hence, the diffuse character of the wide angle reflection in Figure 4 is consistent with the orientation of smectic layers in the fiber-forming process. Furthermore, the fact that the (*hk*O) reflection is at a maximum in quadrant while the layer reflections only appear on the equator strongly suggests that the pattern results from orientation of the layer structure and not from a tendecy of the molecules to orient perpendicular to the direction of draw.

An even more complex behavior of the PEIs **1a**−**h** emerged, when the temperature dependence of the layer distances were examined. In the case of **1d** ($n = 9$) no

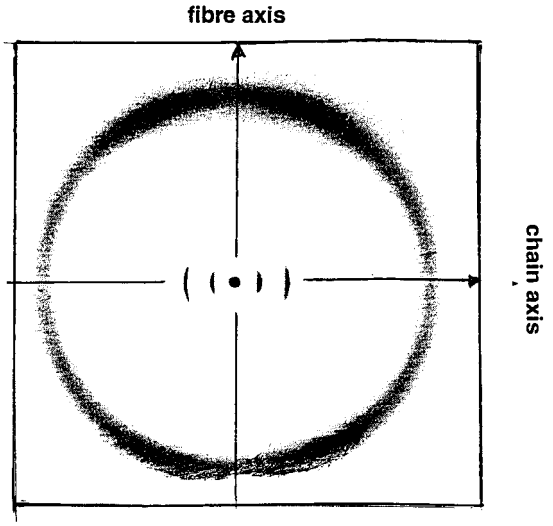

Figure 4. WAXS fiber pattern of PEI **1d** ($n = 9$).

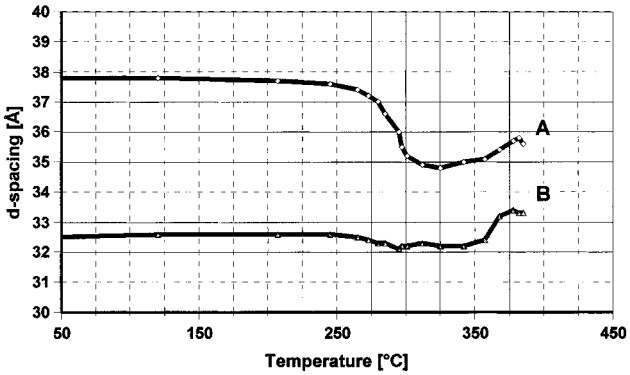

Figure 5. Plot of *d*-spacings versus the temperature: (A) PEI **1a** ($n = 12$); (B) PEI **1d** ($n = 9$).

significant change occurred during the melting process, so that the formation of a smectic-C phase most likely took place above T_m. Yet, when the temperature approached T_i, the layer distance increased and a smectic-A phase was formed. In the case of **1a** the melting was immediately followed by a shrinking of the layer distance (Figure 5A). This shrinking effect was also observed, albeit less pronounced, for **1c** ($n = 10$) and **1e** ($n = 8$). Possibly, the fraction of gauche conformations increases at the expense of the trans conformations. However, such a conformational change cannot explain the extent of this effect and it cannot explain why higher temperature cause again a widening of the layer distance. Therefore, it may be concluded that also the PEIs with even-numbered spacers form a smectic-C phase immediately above T_m, quite analogous to the odd-numbered PEIs. This conclusion was confirmed by X-ray measurements of an oriented sample of **1a** (sheared between glass plates in the smectic LC phase) conducted with synchrotron radiation up to 300 °C (Figure 6). This particular sample of **1a** demonstrates that the chain axis parallels the fiber axis and proves that the mesogens adopt an upright position relation to the layer plane in perfect agreement with the above interpretation of the *d*-spacing (Figure 3). The fiber pattern of another sample of **1a** (with lower molecular weight) showed the chain axis in a perpendicular position relative to the fiber axis quite analogous to the fiber pattern of **1d** in Figure 4. But again no tilting of the mesogens was detectable. However, immediately above T_m a tilting of the mesogens occurred (Figure 6B) which was reversible upon subsequent cooling. Obviously increasing temperature caused a gradual expansion of the layer distances, and finally a smectic-A is formed before the isotropization occurs.

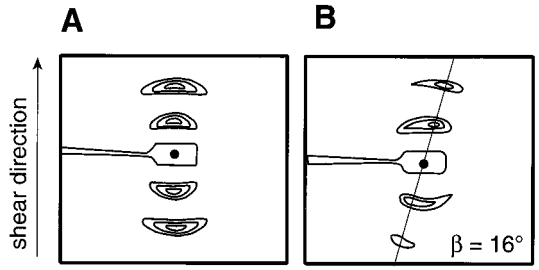

Figure 6. WAXS fiber patterns of PEI **1a**: (A) measured at 25 °C, (B) measured at 300 °C.

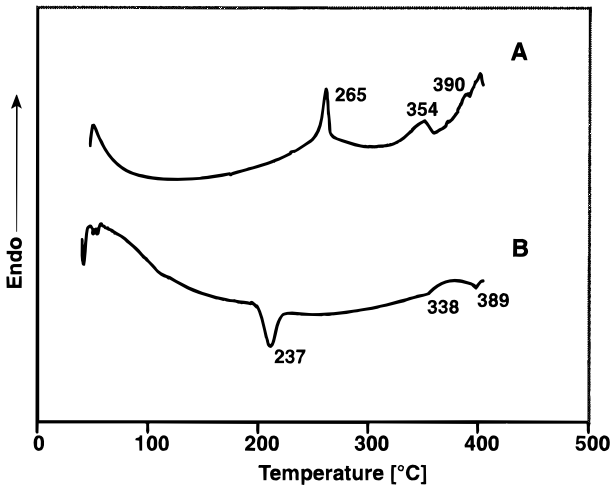

Figure 7. DSC measurements (heating and cooling rate 20 °C/min) of the homo PEI **1a**: (A) first heating; (B) first cooling.

Careful differential scanning calorimetry (DSC) measurements of PEI **1a** revealed three endotherms in the first heating trace (Figure 7A). The first endotherm (265 °C) represents the melting process, i.e., the transition from a smectic-E to the smectic-C phase. A weak broad endotherm at 354 °C fits in with the transitions form the smectic-C to the smectic-A phase postulated by the X-ray measurements. However, the X-ray data of Figure 5 do not show a sharp step indicating a transition from smectic-C to smectic-A. Why this transition appears a little sharper in the DSC trace cannot be explained at this time (it depends, of course, on the heating rate). The third endotherm around 390 °C corresponds to the isotropization process observed by optical microscopy. As demonstrated by the cooling curve of Figure 7 all three transitions are reversible despite the high temperatures. Interestingly a significant supercooling effect is only observable for the low-temperature exotherm, i.e., for the formation of the smectic-E-like solid state. This supercooling effect depends on the cooling rate and suggests the existence of a nucleation process. This finding and the WAXS reflections justify to call the formation of the smectic-E phase a crystallization process. An endotherm indicating the smectic-C to smectic-A transition was barely detectable in the DSC heating trace of **1c** and absent in the DSC trace of **1e**. The thermal degradation hinders in this case and for all PEIs with shorter spacers a satisfactory characterization by DSC measurements.

Taken together, the various X-ray measurements are in satisfactory agreement with both DSC data and optical microscopy. At room temperature even- and odd-numbered PEI adopt two different solid smectic phases,

Table 2. Thermal Properties of Copoly(ester imide)s 2a−h

polym. no.	*n*	T_g[a] (°C)	T_{m1}[a] (°C)	T_{m2}[a] (°C)	T_{i3}[b] (°C)	smectic LC[c] phase(°C)[b]	nem. LC phase(°C)[b]
2a	12	not det.	265	354	385−395	265−395	
2b	11	not det.	286		400−405	290−405	
2c	10	not det.	274	366	390−395	280−395	
2d	9	101	261		375−390	260−390	
2e	8	not det.	287		390−400	290−400	
2f	7	105	253		390−395	265−395	
2g	6	110	290	316	390−400	300−325	325−400
2h	5	122	254	324	390−400	250−320	320−400

[a] From DSC measured with heating rate of 20 °C/min. [b] The isotropization temperatures of these columns are based on optical microscopy. [c] Mainly fan-shaped textures, bâttonet textures were observed immediately before the isotropization or after cooling from the isotropic melt. [d] Not detected.

namely, smectic-E and smectic-H. Obviously the tilted array of mesogens is thermodynamically less stable and, thus, the PEIs **1a**−**h** show a strong odd/even effect of the melting temperatures (Figure 1). However, both series of PEIs form the same kind of LC phases, at lower temperatures a smectic-C and later a smectic-A phase, so that no odd/even effect is observable for T_i.

Copoly(ester imide)s 2b−h. All copoly(ester imide)s **2b**−**h** were prepared in such a way that a mixture of two different imide dicarboxylic acids was polycondensed with 4,4′-bis(acetoxybiphenyl) in bulk at temperatures up to 320 °C. Since the reactivity of the dicarboxyclic acid does not depend on the lengths of the spacers between the imide rings, random sequences of both spacers should have been formed in all cases. This means, that all layers formed by **2b**−**h** either in the solid or in the liquid state necessarily contain both short and long spacers, although in variable molar ratios. The yields, inherent viscosities, and elemental analyses of **2a**−**h** are summarized in Table 1.

The DSC measurements of **2b**−**h** revealed (in agreement with the WAXS patterns discussed below) that all coPEIs like the homoPEIs form a quasi-crystalline solid smectic state. Even after cooling from the isotropic melt with a rate of approximately −300 °C the glass-transitions of noncrystalline phases were difficult to detect. Only in the case of **2d** and **2f**−**h**, where the spacer lengths differ largely, glass-transition temperatures (T_gs) detectable (Table 2). These T_gs increase with decreasing length of the second spacer (i.e., **2d**−**h**). For the melting endotherm (T_{m1} in Table 2) an odd−even effect is evident which is analogous but less pronounced than in the case of the homoPEIs **1a**−**h**. In the case of **2c** a weak endotherm around 366 °C is detectable in the second and third heating curve (T_{m2} in Table 2). It obviously indicates the smectic-C → smectic-A transition in analogy to PEI **1a**/**2a**. An analogous endotherm is absent in the DSC curves of *the* other copoly(ester imide)s. The T_{m2} endotherm of **2g** and **2h** has another origin (see below). The isotropization temperatures (T_i in Table 2) are surprisingly small depending on the variation of the spacers. However, T_i is not clearly detectable in the DSC traces of all PEIs because it is affected by the thermal degradation which is rapid above 390−400 °C. Nonetheless, the thermal stability of all PEIs was high enough for a reliable and reproducible characterization of the textures immediately below T_i.

The textures observed for **2b**−**e** resemble those of **1a**−**h**. A kind of fan-shaped textures was formed by all PEIs immediately above T_{m1}. Yet, when the temperature approached T_i a bâttonet texture such as that of Figure 2A emerged in the case of **2b**−**e** (Figure 2B represents an intermediate state between bâttonets and fans).

A different phase behavior was found for **2g** and **2h**. Due to a sufficient destabilization of the layer structure

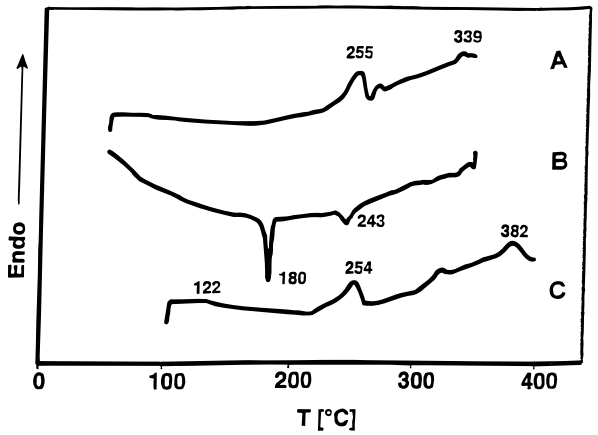

Figure 8. DSC measurements (heating and cooling rate 20 °C/min) of co PEI **2h**: (A) first heating; (B) first cooling; (C) second heating.

these coPEIs finally form a nematic phase as indicated by the typical schlieren texture of Figure 2C. The transition from the smectic-C to the nematic phase occurs in both cases in the temperature range of 330−350 °C, which is evident from microscopic observations but also from a weak endotherm in the second and third heating curve of the DSC measurements (Figure 8). In the case of **2f** the nematic phase is formed immediately below T_i.

All PEIs **2a**−**h** were subjected to X-ray measurements with synchrotron radiation up to 400 °C. Both the middle angle and the wide angle range were recorded and analyzed. Figures 9 and 10 may serve as representative examples of the changes the MARs and wide angle reflections (WARs) undergo during the heating process (heating rate 20 °C/min). The *d*-spacings calculated for 25 °C, immediately above T_{m1} and below T_i are listed together with the phase transition temperatures in Table 3. All measurements have in common that the layer distances shrink above T_{m1} quite analogous to the thermal behavior of the homopolymer **2a** (**1a**) (Figure 9). In the case of **2a**−**e** a gradual increase of the spacing occurs, when the temperature approached T_i. Obviously a smectic-C phase forms first and changes to a smectic-A phase upon further heating. The higher temperatures have the consequence that the intensity of the MARs gradually diminuishes, and in the case of **2f** they disappear around 350 °C (Figure 10). This finding agrees with the observation of a nematic schlieren texture immediately below T_i. In the case of **2g** and **2h** the MARs vanish between 300 and 310 °C (Figure 11) again due to the formation of a nematic phase around 320 °C (Figures 2C and 7). Thus, the synchrotron radiation measurements of the coPEIs **2b**−**h** perfectly agree with the DSC measurements and the microscopic observations, and they also fit in with the

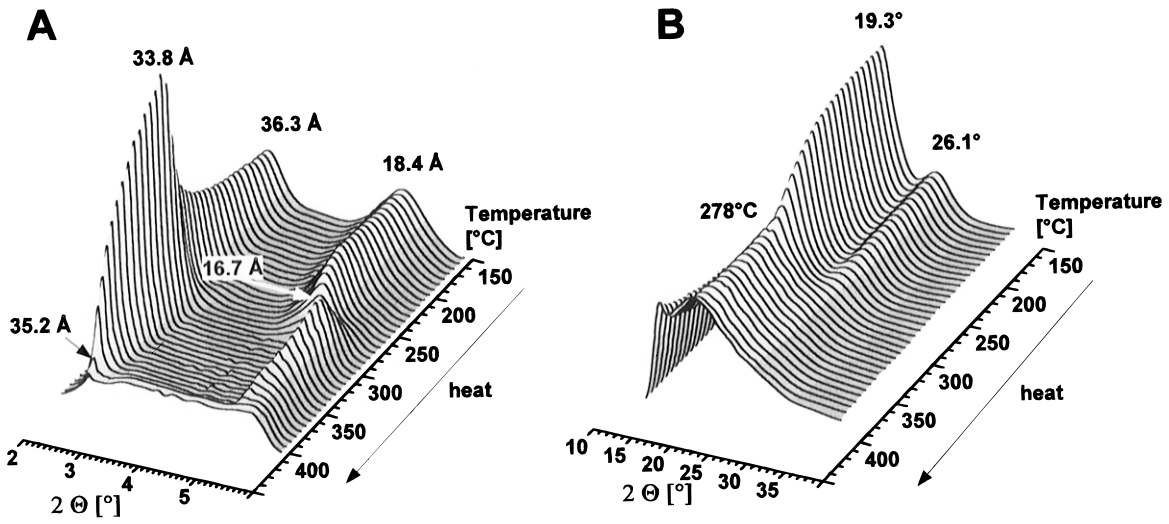

Figure 9. Synchrotron radiation measurements (heating rate 20 °C/min) of coPEI **2c**: (A) middle angle reflection; (B) wide angle reflections.

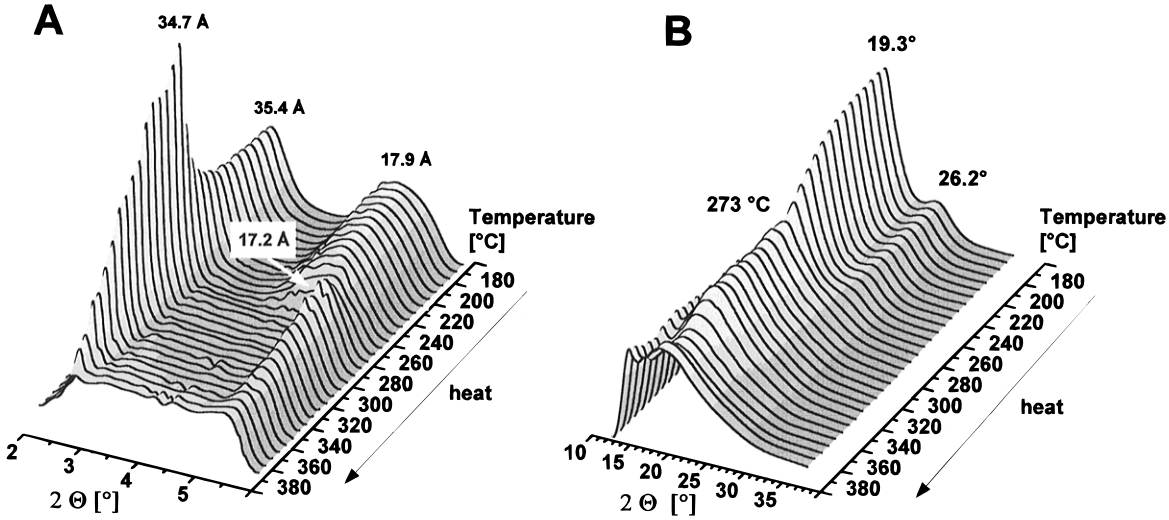

Figure 10. Synchrotron radiation measurements (heating rate 20 °C/min) of coPEI **2f**: (A) middle angle reflections, (B) wide angle reflections.

Table 3. Middle Angle Reflections and *d*-Spacings of the Copoly(ester imide)s 2a−h

polym. no.	*n*	middle angle reflections (Å) 1st order	2nd order	3rd order	4th order	*d*-spacing (Å)	*d*-spacing (Å) of the homopol. **1a−h**
2a	12	36.8	18.8	12.6	9.5	37.5	37.5
2b	11	35.4	17.7		8.8	35.4	33.2
2c	10	36.3	18.3	18.1		36.3	36.5
2d	9	36.4	18.9			36.4	30.7
2e	8	35.6	17.9	10.6	7.7	35.4	32.9
2f	7	35.4	17.9		7.6	35.6	27.4
2g	6	35.4	17.3	10.0	7.6	34.7	31.1
2h	5	35.4	17.6		7.4	35.3	26.5

properties of the homo PEI **1a/2a** as discussed above.

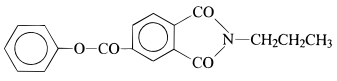

5

Problems of the Chain Packing. This interpretation leaves the following questions open. Why do the PEIs **2a**−**e** form a smectic-C phase between a solid state with upright mesogens and a smectic-A phase with nearly upright mesogens. A partial and hypothetical answer on these questions is based on a computer calculation of a so-called docking experiment. Two *N*-phenylphthalimide groups were endowed with their force fields in a so-called docking-grid and packed together with minimization of the total energy content. The results of these "docking-experiments" are illustrated in Figure 12 examplary for model compound **5** which is a representative segment of the repeating unit of **1g**. The phthalimide groups take on a staggered position with a translation of 0.8 Å in the *z*-direction (long axis) in the case of *N*-phenylphthalimide or 2.4 Å in the case of *N*-propyltrimellitimidephenyl ester (**5**). These results mean that mesogens based on N-substituted phthalimides possess an inherent tendency to adopt a tilted array corresponding to a smectic-C phase

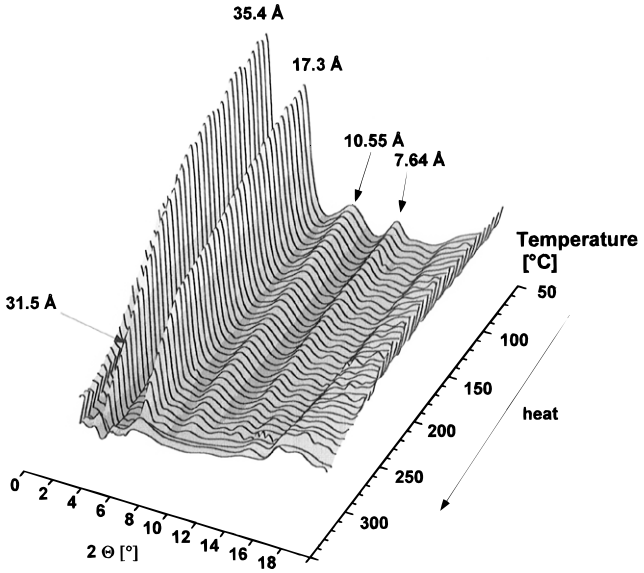

Figure 11. Synchrotron radiation measurements (heating rate 20 °C/min) of coPEI **2g** middle angle reflections).

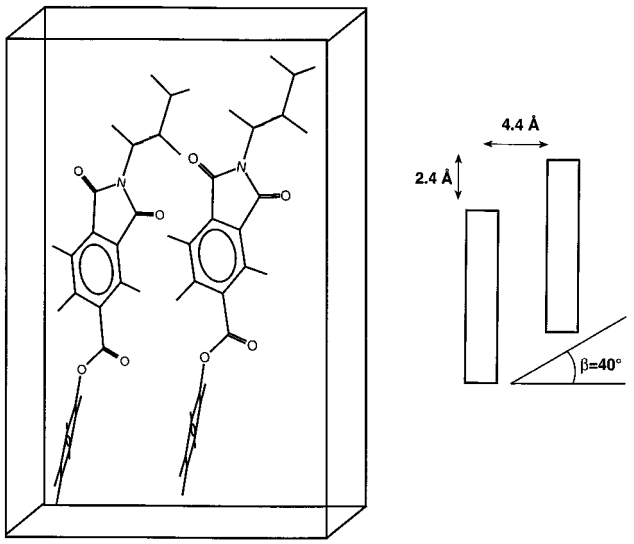

Figure 12. Result of a "docking experiment" with model compound **4**: energy minimum conformations and position of two neighboring molecules.

in the melt or a smectic-F, -G, and -H, phase in the solid state. From this point of view it is not the smectic-C or -H phase but the formation of a smectic-A or -E phase which is the more surprising property of the PEIs **1a**−**h** or **2a**−**h**. However, it must be taken into account that the mesogenic unit of the PEIs **1** or **2** are symmetrical, and thus, the electronic interactions favoring a tilt may cancel each other. Furthermore, the transition to a smectic-A phase with increasing temperature may be favored by two more reasons. Firstly, the X-ray characterization of **2a** (e.g., Figures 5 and 6) indicate that the tilt angle in the melt above T_{m1} is rather small (15−20° relative to the normal on the layer plane). Secondly, increasing temperature accelerates flips and rotational motions of the aromatic rings. There motions may have the consequence that the tilt angle is reduced and randomized in all directions (azimuthal disorder of the tilt direction). A slight tilting with azimuthal disorder of the tilt direction within each layer is consistent with the definition of a smectic-A phase. In fact most semiflexible polyimides described so far form a smectic-A phase below T_i.[14−16]

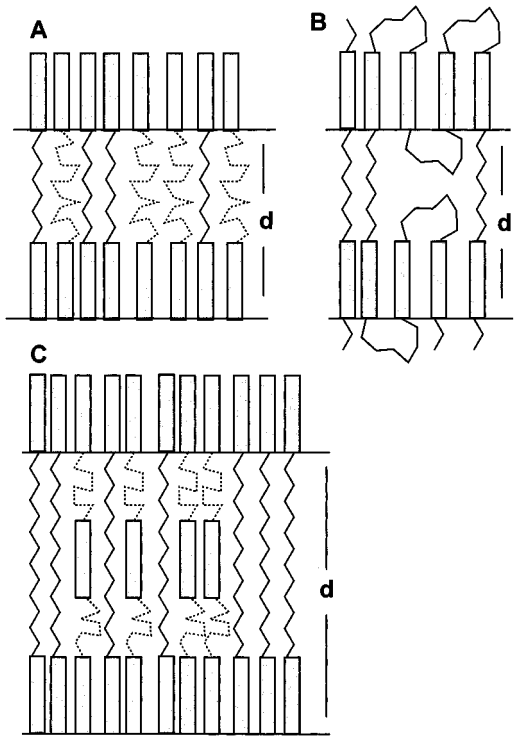

Figure 13. Schemes of layer structures containing spacers of different lengths: (A) the short spacers fully extended; (B) the short spacers forming "loops", (C) the short spacers and attached mesogens dispersed between the fully extended long spacers.

The chain packing in the solid state is, of course, a result of all electronic interactions between neighboring repeating units, and the interaction between the phthalimide groups is not necessarily predominant. Therefore the tilting favored by the phthalimide groups themselves may be outstripped by the sum of all other interactions. The odd−even effect of the *d*-spacings clearly indicates that the spacers have a predominant influence in this case.

The most interesting aspect of the solid state of **2b**−**h** is the finding that both layer distances and chain packing depend very little on the lengths of the spacers (Figure 11 and Table 3). A slight decrease from 37.2 ± 0.2 to 35.0 ± 0.3 Å was found. A *d*-spacing of 35.0 Å fits in with an upright position of the mesogen in combination with a C_{12}-spacer having an equimolar ratio of t and g conformations. For the neat PEI **2a** the X-ray data (e.g., Figure 1) suggest a higher fraction of trans conformations. However, the maximum length of **1h** with fully extended C_5-spacer amounts to 30 Å. Hence the layer distances of **2f**−**h** cannot be confined by the short spacers in an all-trans conformation. For other copoly(ester imide)s containing mixed spacers (e.g., **5a**−**d**) it has indeed been found that the extended short spacers limit the layer distances[5] as illustrated by the scheme of Figure 13A.

Thus, the experimental *d*-spacings of **2f**−**h** raise the interesting question, "where are the short spacers?". In the preceding part of this series another class of coPEIs containing spacers of different lengths was studied and the layer model of Figure 13C was proposed. The relatively short mesogens (when linked to short spacers), may be dispersed in the spacer layer because the long spacers are more than twice as long as the mesogen. However, in the present work the mesogens are longer than the longest spacers, and thus, the layer model of Figure 13C cannot explain the X-ray data of

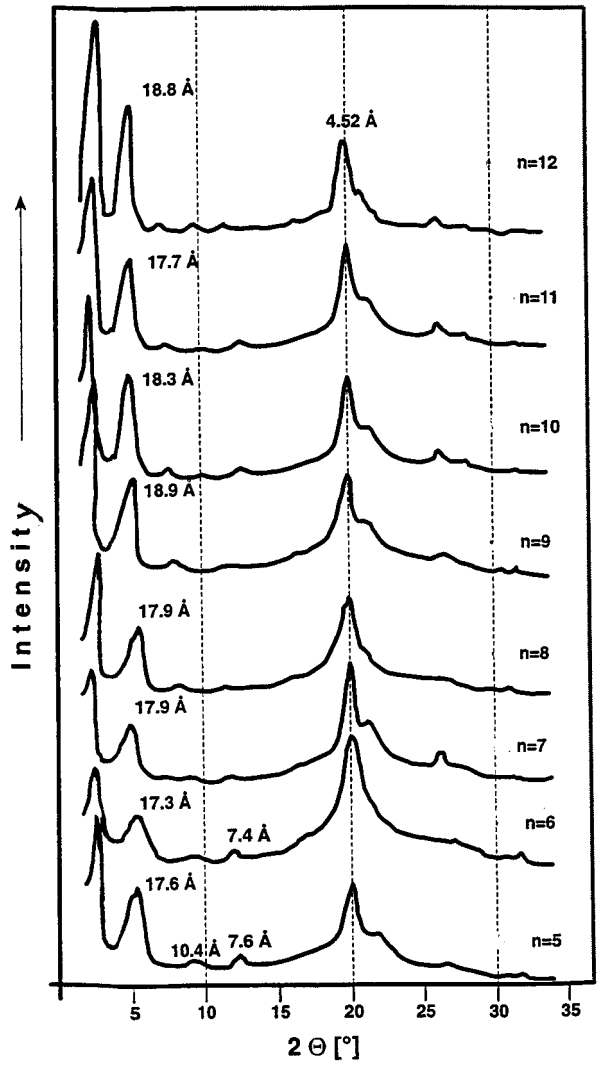

Figure 14. WAXS powder patterns of the poly(ester imide)s **2a**−**h** recorded at 25 °C.

2b−**h**. The only and certainly speculative answer we can offer at this time is the assumption that the short spacers form loops inside the layers and on their surfaces as illustrated in Figure 13B. Such loops affect neither the layer distance nor the lateral packing of the mesogens, and the constancy of these properties is confirmed by the conventional WAXS powder patterns of **2a**−**h** (Figure 14). The loops inside the layers leave more free volume which allows the longer spacers to adopt more gauche conformations and to reduce the layer distance a little relative to **2a**. In other words the scheme of Figure 13B agrees with all experimental data available in this work. In this connection it should be mentioned that several research groups have discussed and demonstrated[17−21] that LC-main chain polyesters containing aliphatic spacers may form folded chain crystals with "loops" of the aliphatic spacers on the long surfaces of the lamellae. Larger loops containing even mesogenic units have also been postulated.[22]

The powder patterns of Figure 14 also indicate that the mesogens do not adopt an exact hexagonal order but an orthorhombic arrangement. With upright mesogens this chain packing may be labeled smectic-E (and with tilted mesogens smectic-H). With this terminology nothing should be said about the three-dimensional order of the mesogens (relative orientation) in subsequent layers. The analysis of the long range order in direction of the chain axis requires a more detailed

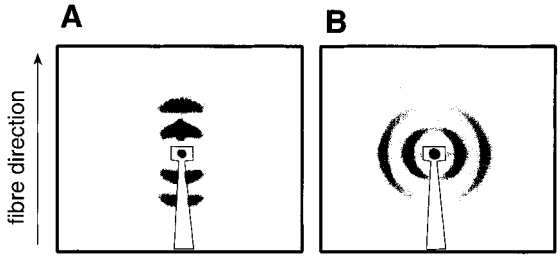

Figure 15. Fiber patterns showing the middle angle reflections of (A) coPEI **2g**, and (B) coPEI **2h**.

X-ray and electron-difraction study which was not intended in this work.

Finally the X-ray fiber patterns of the coPEIs **2b**−**h** need a short comment. As demonstrated by Figure 15 these fiber patterns show that the layer planes either are exactly parallel to the fiber axis or adopt an exactly perpendicular array quite analogous to the fiber patterns of the homoPEI **2a**. Romo-Uribe and Windle have determined the relationship between these two types of orientation to depend on three critical factors: molecular weight, shear rate, and temperature.[23] This finding in combination with the *d*-spacings suggests that the influence of C_{12}-spacer predominates over the shorter spacers even in the case of the odd spacers (**2b**, **2d**, **2f**, **2h**). This result in turn is in perfect agreement with the layer structure of Figure 13B, because the short spacers, when forming loops, will not induce a tilting of the mesogens.

Conclusions

The results of this work confirm our previous study in that the PEIs **1a**−**h** form two different kinds of smectic layer structures in the solid state. With an even number of CH_2 groups the mesogens are in an upright position corresponding to a smectic-E phase. With an odd number of CH_2 groups the mesogens are slightly tilted corresponding to a smectic H structure (the WAXS reflections exclude a heaxagonal packing of the mesogens inside each layer). Upon heating, the PEIs with even-numbered spacers undergo a contraction of the layer distance above the melting temperature T_{m1}. In this way they form a smectic-C phase like the PEIs with odd-numbered spacers. Furthermore, both series of PEIs adopt a smectic-A phase when the temperature approaches T_i.

The co-PEIs containing a C_{12}-spacer in a random combination with a shorter spacer show properties largely resembling those of the homopolymer **2a** (**1a**). The layer distance of the solid phase proved to be rather insensitive to a variation of the shorter spacer, and no satisfactory explanation can be offered, how the short spacers fit into the layer structure. Above T_{m1} again a smectic-C phase is formed which changes to a smectic-A phase at higher temperatures, when the lengths of both sorts of spacers are much different. A greater difference of spacer lengths such as the combinations C_7/C_{12}, C_6/C_{12}, and C_5/C_{12} (**2f**−**h**) results in an appreciable destabilization of the layer structure in the molten state. Whereas, the smectic-C phase is formed even by **2f**−**h**, the smectic-A phase is replaced by a nematic melt.

Particular interesting is a comparison of these results with the properties of other copoly(ester imide)s containing spacers of different length. In the case of **6a**−**d** the variation of the second spacer has no appreciable influence on the thermal properties. The co PEIs **6b**−**d** form a monotropic smectic-A phase upon cooling quite

analogous to their parent homoPEIs. The homoPEIs of structure **7** with long spacers (e.g., **7a**) form a monotropic nematic phase. The combination of a long and a short spacer (**7b**−**d**) has here the consequence that an enantiotropic nematic phase can exist over a narrow temperature range (5−10 °C). This comparison demonstrates that the response of layer structures to a combination of different spacers depends very much on the chemical structure of the individual polymer. At this time no rules exist allowing reliable predictions. Another interesting aspect of the present and previous studies[5,6] is the necessity to formulate new types of smectic layer structures (Figure 13A−C) which have no counterparts in the field of low molar mass smectogens or smectic-LC-side chain polymers.

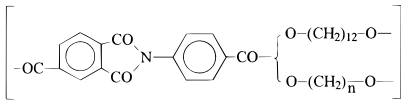

6

a: n = 12 b: n = 10
c: n = 9 d: n = 8

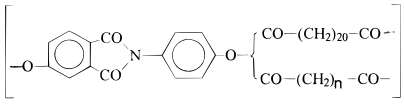

7

a: n = 20 b: n = 12 c: n = 7

References and Notes

(1) Kricheldorf, H. R.; Pakull, R. *Macromolecules* **1988**, *21*, 551.
(2) Kricheldorf, H. R.; Pakull, R. *Polymer* **1987**, *28*, 1773.
(3) Kricheldorf, H. R. *Mol. Cryst. Liq. Cryst.* **1994**, *254*, 87.
(4) de Abajo, J.; de la Campa, J.; Kricheldorf, H. R.; Schwarz, G. *Polymer* **1994**, *35*, 5577.
(5) Kricheldorf, H. R.; Schwarz, G.; Berghahn, M.; de Abajo, J.; de la Campa, J. *Macromolecules* **1994**, *27*, 2540.
(6) Kricheldorf, H. R.; Probst, N.; Schwarz, G.; Wutz, C. *Macromolecules* **1996**, *29*, 4234.
(7) Roviello, A.; Sirigu, A. *Eur. Polym. J.* **1979**, *15*, 61.
(8) Koide, N.; Ohta, R.; Imura, K. *Polym. J.* **1984**, *16*, 505.
(9) Kwon, S. K.; Chung, I. J. *Eur. Polym. J.* **1994**, *30*, 1081.
(10) Watanabe, J.; Nakata, Y.; Simizu, K. *J. Phys. II.* **1994**, *4*, 581.
(11) Nakata, Y.; Shimizu, K.; Watanabe, J. *High Perform. Polym.* **1995**, *7*, 377.
(12) Watanabe, J., Krigbaum, W. R.; Macromolecules **1984**, *17*, 2288.
(13) Leland, M.; Wu, Zi; Chhajer, M.; Ho-R.; Cheng, S. Z. D.; Keller, A.; Kricheldorf, H. R. Manuscript in preparation.
(14) Pardey, R.; Wa, S. S.; Chen, J.; Harris, F. W.; Cheng, S. Z. D.; Keller, A.; Aducci, J.; Facinelli, J. V.; Lens, R. W. *Macromolecules* **1994**, *27*, 5794.
(15) Kricheldorf, H. R.; Linzer, V. *Polymer* **1995**, *36*, 1893.
(16) Kricheldorf, H. R.; Gurau, M. *J. Polym. Sci., Part A, Polym. Chem.* **1995**, *33*, 2241.
(17) Thomas, E. L.; Wood, B. A. *Faraday Discuss. Chem. Soc.* **1985**, *79*, 229.
(18) Takahashi, T.; Nagata, F. *J. Macromol. Sci., Phys. B* **1989**, *28*, 349.
(19) Hudson, S. D.; Thomas, E. L.; Lenz, R. W. *Mol. Cryst. Liq. Cryst.* **1987**, *153*, 63.
(20) Olbrich, E.; Chen, D.; Zachmann, H. G. *Macromolecules* **1991**, *24*, 4364.
(21) Kent, S. L.; Geil, P. H. *J. Polym. Sci. Part B., Polym. Phys.* **1992**, *30*, 1489.
(22) Tokita, M.; Takahashi, T.; Hayashi, M.; Inomata, K.; Watanabe, I. *Macromolecules* **1996**, *29*, 1345.
(23) Romo-Uribe, A.; Windle, A. H. *Macromolcules* **1997**, *29*, 6246.

MA960921N